

Benchmark of TJ Code Against STRIDE Code

R. Fitzpatrick ^a

*Institute for Fusion Studies, Department of Physics,
University of Texas at Austin, Austin TX 78712, USA*

I. SYMMETRY RELATIONS

Let all lengths be normalized to the major radius of the magnetic axis, R_0 , and let all magnetic field-strengths be normalized to the toroidal magnetic field-strength at the axis, B_0 . Consider an axisymmetric toroidal plasma equilibrium. Let R, ϕ, Z be a conventional cylindrical coordinate system that is co-axial with the toroidal symmetry axis of the plasma. The equilibrium magnetic field is written

$$\mathbf{B} = \nabla\phi \times \nabla\psi + g(\psi) \nabla\psi, \quad (1)$$

where ψ is the poloidal magnetic flux. We can also define

$$\Psi_N = \frac{\psi}{\psi_a}, \quad (2)$$

where ψ_a is the poloidal flux at the plasma boundary. Thus, $\Psi_N = 0$ at the magnetic axis, and $\Psi_N = 1$ on the plasma boundary. In the following, it is assumed that Ψ_N is the ‘radial’ coordinate in STRIDE.

Let

$$L_m^m(\Psi_N) = I(\Psi_N) \left(J(\Psi_N) \left[\frac{m g(\Psi_N)}{q(\Psi_N)} \right]^2 + [n \psi_a]^2 \right), \quad (3)$$

$$I(\Psi_N) = \int_0^{\Psi_N} \frac{2 q(\Psi'_N)}{g(\Psi'_N)} d\Psi'_N, \quad (4)$$

$$J(\Psi_N) = \oint |\nabla\Psi_N|^{-2} \frac{d\theta}{2\pi}, \quad (5)$$

$$\rho(\Psi_N) = \frac{J(\Psi_N) g(\Psi_N)}{q(\Psi_N)}, \quad (6)$$

$$s(\Psi_N) = \frac{d \ln q}{d\Psi_N}, \quad (7)$$

^a rfitzp@utexas.edu

where m is a poloidal mode number, n is a toroidal mode number, $q(\Psi_N)$ is the safety-factor, and θ is a ‘straight’ poloidal angle defined such that

$$(\nabla\phi \times \nabla\theta \cdot \nabla\phi)^{-1} = \frac{qR^2}{g}, \quad (8)$$

Note that we are working in PEST coordinates.

Let m_j be the poloidal mode number of the j th rational surface, which is located at $\Psi_N = \Psi_{Nj}$. Let D_{Ij} be the ideal Mercier index at the j th rational surface, and let

$$\nu_{Lj} = \frac{1}{2} - \sqrt{-D_{Ij}}, \quad (9)$$

$$\nu_{Sj} = \frac{1}{2} + \sqrt{-D_{Ij}}. \quad (10)$$

Let

$$f_{Lj} = \left[\rho^{\nu_{Lj}} \left(\frac{\nu_{Sj} - \nu_{Lj}}{L_{m_j}^{m_j}} \right)^{1/2} s m_j \right]_{\Psi_{Nj}}, \quad (11)$$

$$f_{Sj} = \left[\rho^{\nu_{Sj}} \left(\frac{\nu_{Sj} - \nu_{Lj}}{L_{m_j}^{m_j}} \right)^{1/2} s m_j \right]_{\Psi_{Nj}}. \quad (12)$$

Finally, let

$$\hat{A}_{ij} = f_{Sj}^{-1} A_{ij} f_{Lj}, \quad (13)$$

$$\hat{B}_{ij} = f_{Sj}^{-1} B_{ij} f_{Lj}, \quad (14)$$

$$\hat{\Gamma}_{ij} = f_{Sj}^{-1} \Gamma_{ij} f_{Lj}, \quad (15)$$

$$\hat{\Delta}_{ij} = f_{Sj}^{-1} \Delta_{ij} f_{Lj}, \quad (16)$$

where A_{ij} , B_{ij} , Γ_{ij} , and Δ_{ij} are the elements of the outer matching matrices calculated by STRIDE, whereas the hatted quantities are the corresponding matching matrices calculated by TJ. Equations (77) and (100) of Ref. 1 imply that

$$\hat{A}_{ji}^* = \hat{A}_{ij}, \quad (17)$$

$$\hat{\Delta}_{ji}^* = \hat{\Delta}_{ij}, \quad (18)$$

$$\hat{B}_{ji}^* = \hat{\Gamma}_{ij}. \quad (19)$$

These symmetries are ultimately due to the self-adjoint nature of the ideal-MHD force operator. However, as explained in Ref. 2, the symmetries can also be related to the conservation

of toroidal electromagnetic angular momentum. The symmetries have to be respected by a toroidal tearing mode code, otherwise the code would predict that an isolated plasma could exert a net toroidal electromagnetic torque on itself. Note that, in the cylindrical limit, $\hat{\Delta}_{jj}$ is equivalent to $r_s \Delta'$: i.e., the tearing stability index normalized to the minor radius of the rational surface.

II. TJ CIRCULAR EQUILIBRIUM

The TJ circular equilibrium is characterized by a pressure profile

$$p(r) = \beta_0 \left[1 - \left(\frac{r}{a} \right)^2 \right]^{p_p}, \quad (20)$$

and a parallel current profile, $\sigma = \mathbf{J} \cdot \mathbf{B}/B^2$,

$$\sigma(r) = \sigma_0 \left[1 - \left(\frac{r}{a} \right)^2 \right]^{p_\sigma}. \quad (21)$$

These profiles differ from the existing `lar` module in STRIDE because of the $(r/a)^2$, rather than (r/a) , factors in the profiles.

III. BENCHMARK TESTS

A. Single Rational Surface

We use a zero-pressure, circular cross-section, plasma equilibrium that, in the cylindrical limit, has a Wesson-like current profile³ characterized by the safety-factor on the magnetic axis, q_0 , and the safety-factor at the plasma boundary, q_a . In fact, in the cylindrical limit, $j_\phi(r) = (2/q_0) (1 - r^2)^{q_a/q_0}$. We consider the stability of $n = 1$ tearing modes, and consider equilibria that only contain a single $n = 1$ rational surface: namely, the 2/1 surface.

1. Test 1

The first test has $q_0 = 1.1$, $q_a = 2.6$, and varies the inverse aspect-ratio of the plasma, ϵ_a . Figure 1 compares the $\hat{\Delta}_{11}$ (i.e., the tearing stability index of the 2/1 tearing mode) values calculated by the TJ code,⁴ the TEAR code (which is a cylindrical tearing mode code), and the STRIDE code. It can be seen that the tearing stability index calculated by the TJ

code asymptotes to that calculated by the TEAR code in the cylindrical limit, $\epsilon_a \rightarrow 0$. On the other hand, the stability index calculated by STRIDE exhibits wild oscillations in the cylindrical limit, and only becomes believable when $\epsilon_a > 0.2$. In the latter case, the STRIDE and TJ codes exhibit good agreement. Note that TJ has a dud data point at $\epsilon_a = 0.12$, which is under further investigation.

2. Test 2

The second test has $q_0 = 1.1$ and $\epsilon_a = 0.05$, and varies q_a . Figure 2 compares the $\hat{\Delta}_{11}$ values calculated by the TJ code, the TEAR code and the STRIDE code. It can be seen that the tearing stability indices calculated by the TJ and TEAR codes agree with one another, as should be the case in a large aspect-ratio plasma. On the other hand, the tearing stability index calculated by the STRIDE code exhibits significant oscillations about the (presumably) correct answer.

3. Test 3

The third test is the same as the second, except that we have increased ϵ_a to 0.2, because Fig. 1 suggests that STRIDE is more likely to give reliable results at this aspect-ratio. Figure 3 compares the $\hat{\Delta}_{11}$ values calculated by the TJ code, the TEAR code and the STRIDE code. It can be seen that the tearing stability indices calculated by TJ and STRIDE are in reasonably good agreement with one another. Note that the plasma approaches an ideal stability limit as $q_a \rightarrow 3$. Nevertheless, the STRIDE results still exhibit oscillations about the TJ results.

4. Test 4

The fourth test shows the elements of the 2×2 tearing stability index when q_a lies between 2 and 3. It can be seen that TJ and STRIDE are in reasonably good agreement. However, STRIDE is not respecting the symmetry constraints as well as TJ.

REFERENCES

- ¹ A. Pletzer, A. Bondeson, and R.L. Dewar, J. Comp. Phys. **115**, 530 (1994).
- ² R. Fitzpatrick, Phys. Plasmas **1**, 3308 (1994).
- ³ J.A. Wesson, Nucl. Fusion **18**, 87 (1978).
- ⁴ R. Fitzpatrick, Phys. Plasmas **31**, 102507 (2024).

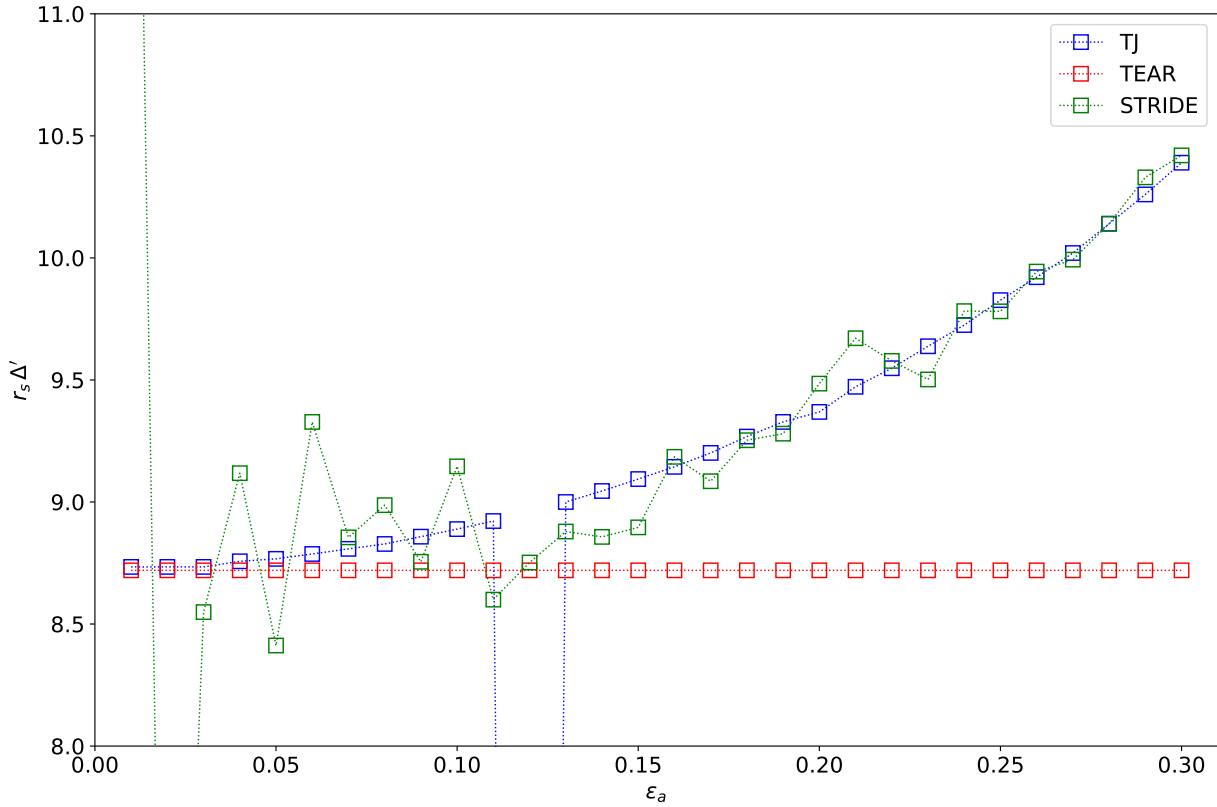


FIG. 1. Test 1: $q_0 = 1.1$, $q_a = 2.6$. Variation of 2/1 tearing stability index with inverse-aspect ratio.

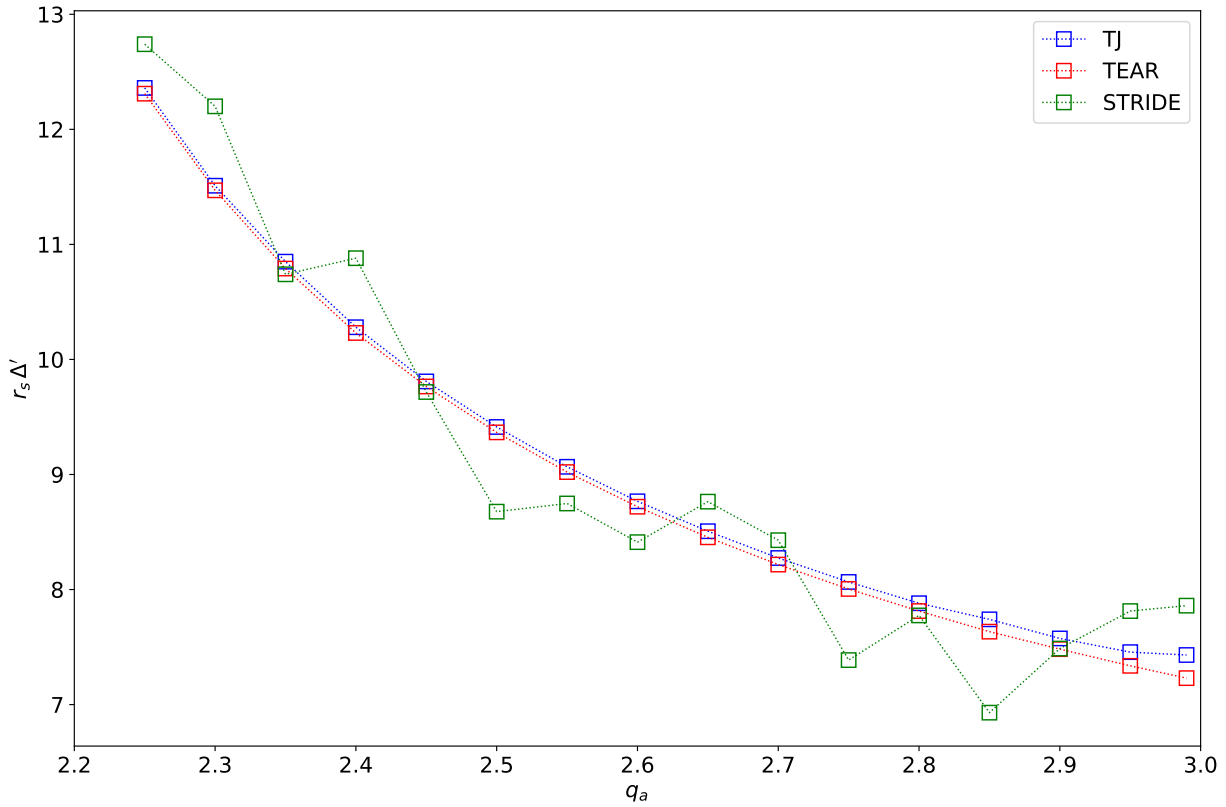


FIG. 2. Test 2: $q_0 = 1.1$, $\epsilon_a = 0.05$. Variation of 2/1 tearing stability index with edge safety-factor.

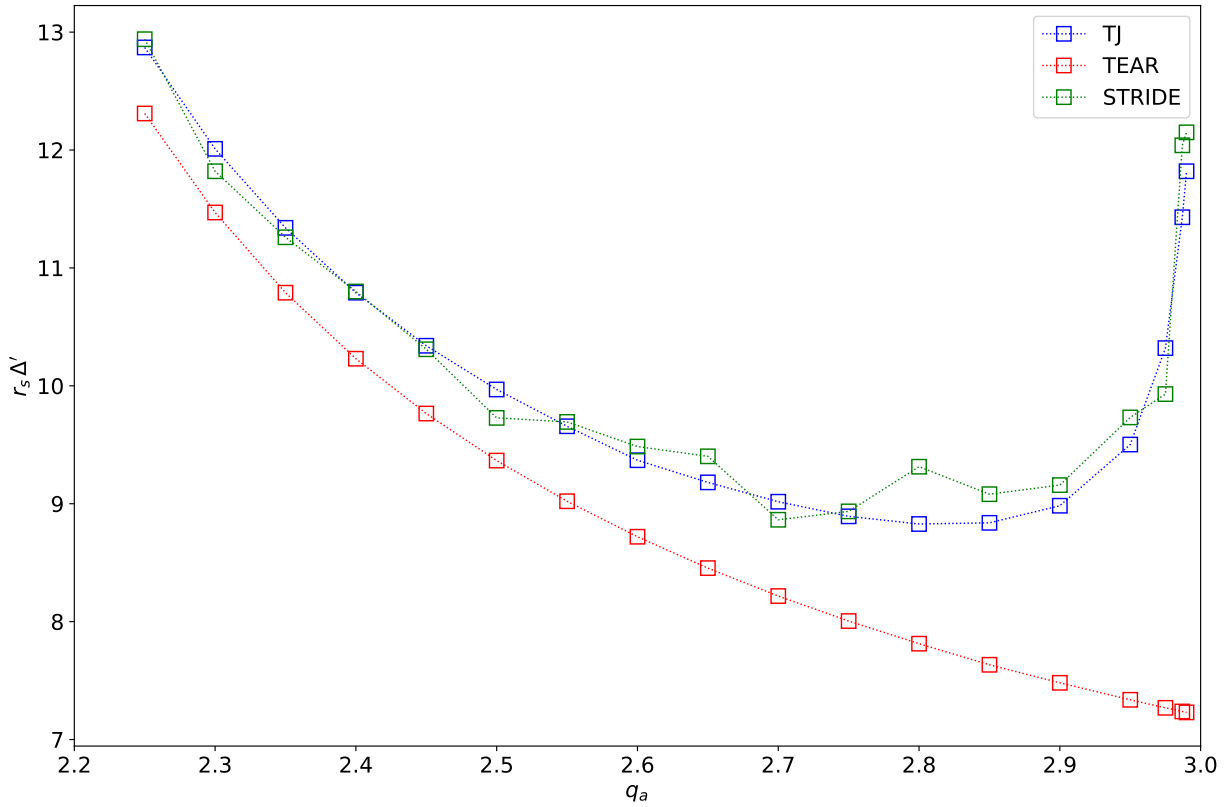


FIG. 3. Test 3: $q_0 = 1.1$, $\epsilon_a = 0.2$. Variation of 2/1 tearing stability index with edge safety-factor.

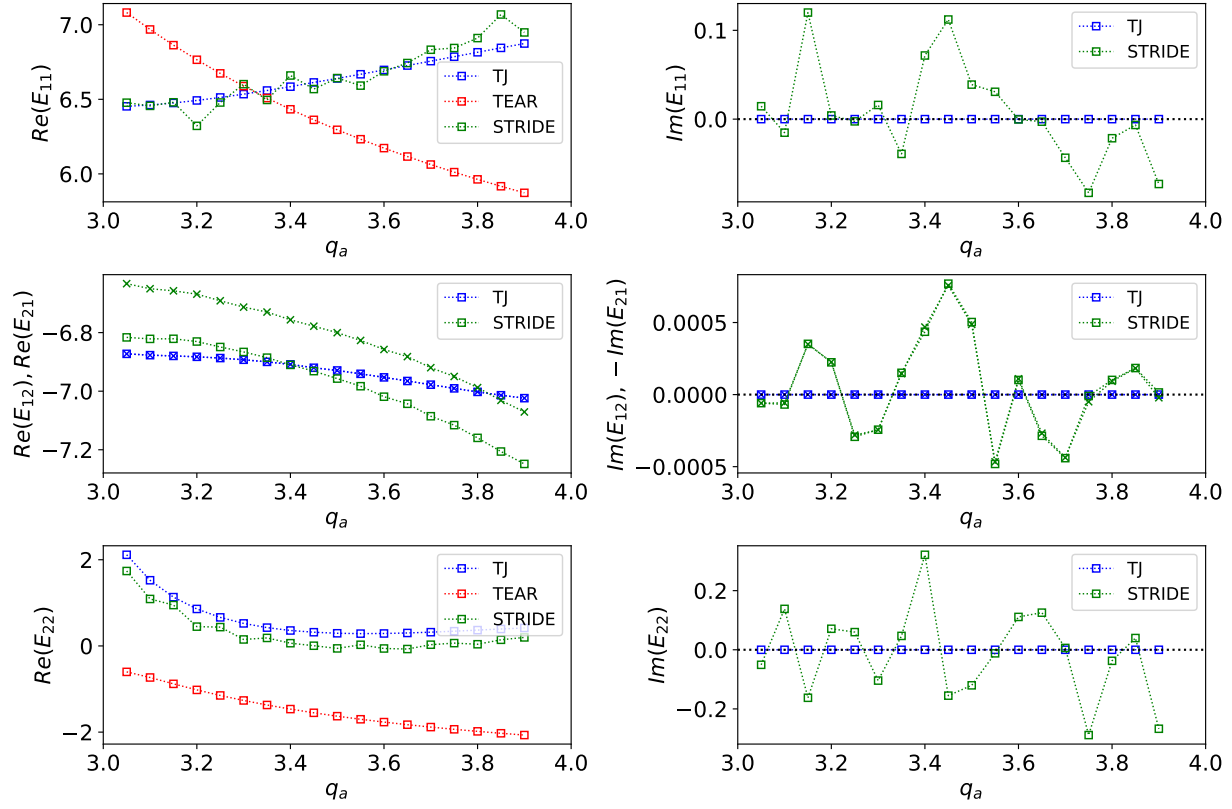


FIG. 4. Test 4: $q_0 = 1.1$, $\epsilon_a = 0.3$. Variation of elements of tearing stability matrix with edge safety-factor.